

# Ultrafast Dynamics of Photogenerated Holes at a CH<sub>3</sub>OH/TiO<sub>2</sub> Rutile Interface

## Supporting Information

Weibin Chu,<sup>1</sup> Wissam A. Saidi,<sup>2</sup> Qijing Zheng<sup>1\*</sup>, Yu Xie, Zhenggang Lan<sup>3,4</sup>, Oleg V. Prezhdo,<sup>5</sup>  
Hrvoje Petek,<sup>6</sup> and Jin Zhao<sup>1,6,7\*</sup>

<sup>1</sup>*ICQD/Hefei National Laboratory for Physical Sciences at Microscale, and Key Laboratory of Strongly-Coupled Quantum Matter Physics, Chinese Academy of Sciences, and Department of Physics, University of Science and Technology of China, Hefei, Anhui 230026, China*

<sup>2</sup>*Department of Mechanical Engineering and Materials Science, University of Pittsburgh, Pittsburgh, Pennsylvania 15261, United States*

<sup>3</sup>*Key Laboratory of Biobased Materials, Qingdao Institute of Bioenergy and Bioprocess Technology, Chinese Academy of Sciences, Qingdao, Shandong 266101, China*

<sup>4</sup>*University of Chinese Academy of Sciences, Beijing 100049, China*

<sup>5</sup>*Departments of Chemistry, and Physics and Astronomy, University of Southern California, Los Angeles, CA 90089, United States*

<sup>6</sup>*Department of Physics and Astronomy, University of Pittsburgh, Pittsburgh PA 15260, United States*

<sup>7</sup>*Synergetic Innovation Center of Quantum Information & Quantum Physics, University of Science and Technology of China, Hefei, Anhui 230026, China*

### 1. Electronic structure for different K sampling

In order to whether the sampling at  $\Gamma$  point is efficient for the electronic structure calculation, we compare the DOS obtained by  $(8\times 8\times 1)$  k-point sampling and only the  $\Gamma$  point. As shown in

Figure S1, for all the adsorption structure M, HD and D, different k-point sampling give qualitatively similar DOS. The band gap increases from 1.5 eV to 1.7 eV when the k-point sampling changes from single  $\Gamma$  point to  $(8 \times 8 \times 1)$  k-point.

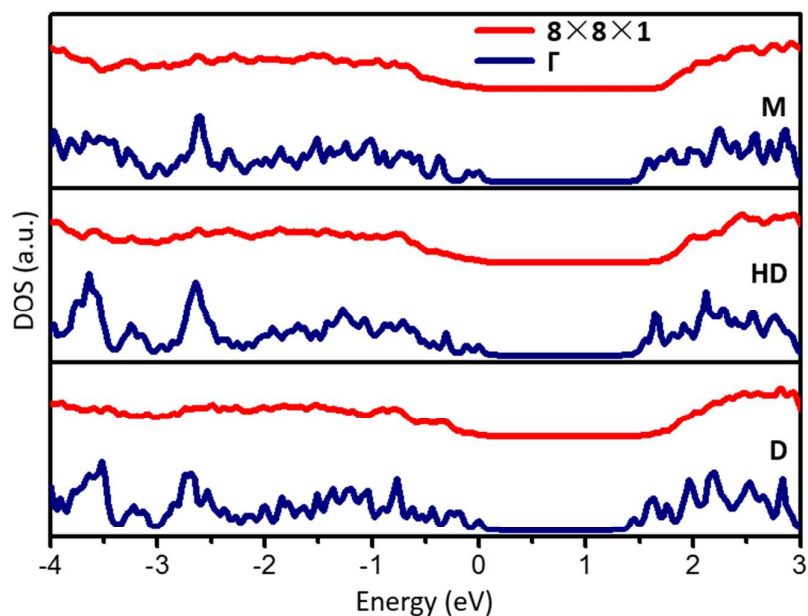


Figure S1. The DOS of M, HD and D structures obtained by single  $\Gamma$  point and  $(8 \times 8 \times 1)$  k-point.

## 2. Electronic structure by DFT+U

The self-interaction errors in DFT may have important effects on the electronic structure of  $\text{TiO}_2$ /molecule interface. We have already compared our DFT results with the GW calculations showing that the difference is negligible.<sup>10</sup> To confirm this point, we performed a PBE+U electronic calculation with  $U=4$  eV for M structure as shown in Figure S2. It is shown that the energy level alignment between  $\text{CH}_3\text{OH}$  with  $\text{TiO}_2$  almost keeps unchanged comparing with PBE calculations, showing that DFT calculations are sufficient.

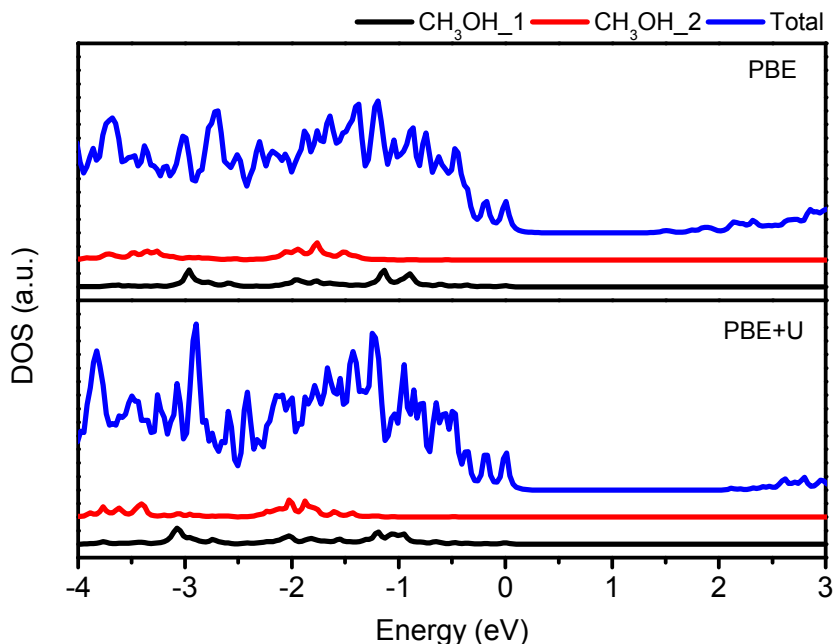


Figure S2. The total and partial DOS of M structure obtained by PBE and PBE+U ( $U=4$  eV).

### 3. Effects of the dangling bonds

In a slab-supercell approach, the effects of the bottom unsaturated dangling bonds on the electronic structure are severe. To remedy this, we saturate the dangling bonds of the bottom layer with pseudo-hydrogen atoms.<sup>1</sup> To illustrate the effect of the unsaturated bonds on the electronic band structure of the system, we show in Figure S2 the projected density of states (DOS) of the fully dissociated  $\text{CH}_3\text{OH}$  structure for each layer. From Figure S2 (a) it is evident with the dangling bonds there exists an artificial interlayer electric field, as suggested by the blue dashed line, which shifts the DOS of each lower layer upwards, and localizes the valence band maximum (VBM) at the bottom layer. By contrast, in Figure S2 (b), after saturation, the artificial interlayer electric field is successfully eliminated and the layer projected density of states of the bottom layer has similar structure to that of the bulk layers.

The saturation of the bonds also helps to decrease finite size effects due to the finite slab thickness, and hence allows us to perform the NAMD calculations for smaller unit cells. To verify this, we calculated the binding energy of the fully dissociated structure computed for different values of the slab thickness. Compared with our previous work without pseudo hydrogen saturation<sup>2</sup>, the molecular adsorption energy converges faster (Figure S2 (c)) with the termination.

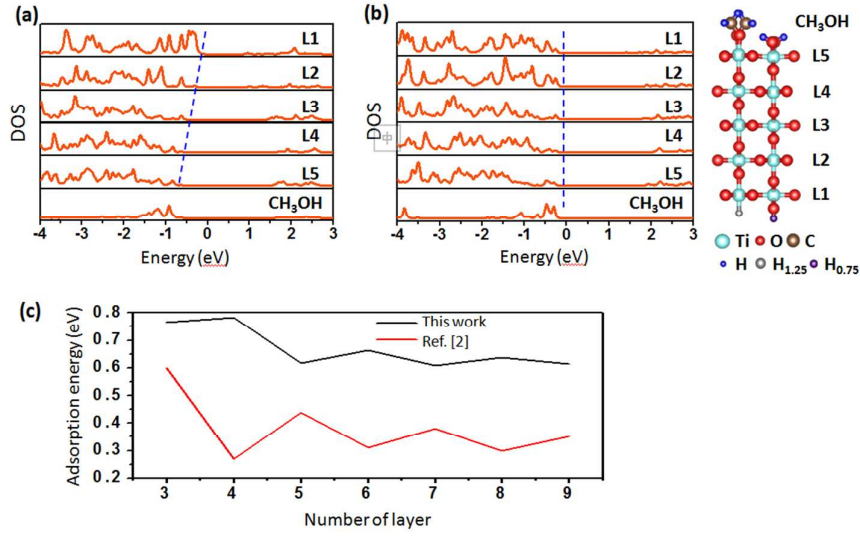


Figure S3. (a-b) The partial DOS of every layer and the adsorbed molecules with and without pseudo H saturation. (c) The adsorption energy dependence on the slab thickness. The black line presents the results in this report while the red line is from ref. [2].

#### 4. Nonadiabatic molecular dynamics with time-domain density functional theory

We applied *ab initio* nonadiabatic molecular dynamics (NAMD) implemented within time domain density functional theory (TD-DFT) in the Kohn-Sham (KS) framework to model the photo-generated hole dynamics. The Runge-Gross theorem asserts that all observables are determined with the knowledge of the one-body electron density. TDDFT in the Kohn-Sham approach maps an interacting many-body system onto a system of noninteracting particles where the electron density of the latter equals to the former. The time-dependent charge density of the interacting system can thus be obtained from the time-dependent KS orbitals,  $\psi_p(r, t)$  as:

$$\rho(r, t) = \sum_{p=1}^{N_e} |\psi_p(r, t)|^2 \quad (1)$$

The evolution of the electron density is determined by the TD variational principle, leading to a set of single-electron equations for the evolution of the KS orbitals:

$$i\hbar \frac{\partial \psi_p(r, t)}{\partial t} = H(r; R) \psi_p(r, t); p = 1, 2, \dots, N_e \quad (2)$$

By expanding the time-dependent KS orbitals in the adiabatic KS orbital basis,  $\phi_p(r; R)$ , which is calculated with time-independent DFT from the geometry in the adiabatic MD as shown below:

$$\psi_p(r, t) = \sum_k c_k(t) \phi_k(r; R) \quad (3)$$

And by inserting Eq.3 into Eq. 2, one can obtain equations for the expanding coefficients:

$$i\hbar \frac{\partial}{\partial t} c_j(t) = \sum_k c_k(t) (\epsilon_k \delta_{jk} + d_{jk}) \quad (4)$$

where  $\epsilon_k$  is the energy of the adiabatic state  $k$ , and  $d_{jk}$  is the non-adiabatic couplings between the basis  $j$  and  $k$ .

The extent of hole transfer between TiO<sub>2</sub> and adsorbed molecules is computed by integrating the projected hole density on TiO<sub>2</sub>.

$$\int_{\text{TiO}_2} \rho_{PE}(r, t) dr = \int_{\text{TiO}_2} |\psi_{PE}(r, t)|^2 dr = \sum_{i,j} c_i^*(t) c_j(t) \int_{\text{TiO}_2} \phi_i^*(r, R(t)) \phi_j(r, R(t)) dr \quad (5)$$

Taking the time-derivative of eq (5) gives the expression for adiabatic (AD) and non-adiabatic (NA) contributions to charge transfer:

$$\frac{d \int_{\text{TiO}_2} \rho_{PE}(r, t) dr}{dt} = \sum_{i,j} \left\{ \frac{d(c_i^* c_j)}{dt} \int_{\text{TiO}_2} \phi_i^* \phi_j dr + c_i^* c_j \frac{d \int_{\text{TiO}_2} \phi_i^* \phi_j dr}{dt} \right\} \quad (6)$$

The change in the charge density described by the first term on the right-hand side of eq (6) is due to change of state occupations of the adiabatic KS states, which we refer to as nonadiabatic transfer term. On the other hand, the second term causes change of charge density by change of localization of the KS adiabatic states, hence the name adiabatic transfer. The contribution to the total charge transfer was obtained by further integrating the two terms on the right-hand side of eq (6).

1. Kowalski, P. M.; Meyer, B.; Marx, D. *Phys. Rev. B* **2009**, 79, (11), 115410-16.
2. Zhao, J.; Yang, J.; Petek, H. *Phys. Rev. B* **2009**, 80, (23), 235416-11.